Structure and Polymorphism of 1,2-Dioleoyl-3-acyl-*sn*-glycerols. Three- and Six-Layered Structures†

David A. Fahey, Donald M. Small,* Dharma R. Kodali, David Atkinson,‡ and Trevor G. Redgrave

Biophysics Institute, Departments of Medicine and Biochemistry, Boston University School of Medicine, Housman Medical Research Center, Boston, Massachusetts 02118

Received December 18, 1984

ABSTRACT: Triacylglycerols, which usually contain at least one unsaturated fatty acid, are the most important forms of stored biological lipids in teleosts, mammals, and most plants. Since the physical properties of such mixed-chain triacylglycerols are poorly understood, a systematic study of such compounds has been initiated. Stereospecific 1,2-dioleoyl-3-acyl-*sn*-glycerols were synthesized with even carbon saturated fatty acyl chains of 14–24 carbons in length. Their polymorphic behavior was examined by differential scanning calorimetry and X-ray powder diffraction. The thermal behavior revealed from one to four major polymorphic transitions depending upon saturated chain length. Plots of enthalpy of fusion and entropy vs. carbon number for melting of the most stable polymorph were linear throughout the series with slopes of 1.0 kcal/mol per carbon atom and 2.6 cal/(mol K) per carbon atom, respectively. These slopes indicate that the saturated chains are packed in a well-ordered tightly packed lattice. When the compounds were rapidly cooled to 5 °C, X-ray powder diffraction revealed strong β' (ca. 3.8 and 4.2 Å) reflections and weak β (ca. 4.6 Å) reflections. The β subcell reflections intensified when the compounds were heated to within 5 °C of the melting temperature of the highest melting polymorph. Evidence of an α phase was not seen on 30-min X-ray exposures for any of the compounds. In the proposed packing arrangement the saturated and unsaturated chains are segregated into layers. The stable form of all compounds exhibits a triple layer packing mode in which a bilayer of oleoyl chains is segregated from an interdigitated layer of saturated chains. The thickness of the glycerol backbone normal to the base plane is about 4.1 Å. The saturated chains are tilted 55.8° with respect to the base plane. This tilt is close to the value of 56.5° obtained from the single crystal study of oleic acid, which may indicate that the saturated chains project from the glycerol backbone like a linear extension of the first nine carbons of the oleoyl chain. In addition, a metastable six-layer packing mode was identified for 1,2-dioleoyl-3-myristoyl-*sn*-glycerol. While some of the complex polymorphisms involve adjustments in chain packing, others may relate to transitions from unstable six-layer to stable three-layer structures.

Acylglycerols are key molecules in lipid metabolism. Triacylglycerols, in which all three hydroxyls of the glycerol are esterified to fatty acids, represent the major storage lipid of higher animals and most plants. Most naturally occurring triacylglycerols show optical activity, indicating that the specific distributions of fatty acids at the 1- and 3-positions are different. Furthermore, most naturally occurring triacylglycerols have at least one and often two unsaturated fatty acids. A specific triacylglycerol structure has important implications for the physical properties of the triacylglycerols (Small, 1985a) and also perhaps for physiological characteristics such as enzyme hydrolysis and subsequent metabolism (Morley et al., 1974). A characteristic feature of triacylglycerols in the solid state is polymorphism because of the possibility of many different packing arrangements of similar lattice energy. This polymorphism has been the subject of numerous studies by different workers extending almost over a century [see reviews by Bailey (1950), Chapman (1962), Lutton (1950), Malkin (1954), and Small (1985a)]. In most earlier studies of triacylglycerols racemic mixtures were studied; however, properties of the racemic mixtures are not necessarily the same as those of the specific isomers (Larsson, 1964).

We have begun a systematic study of a variety of homologous series of optically active triacylglycerols. In our first study we reported the synthesis and polymorphism of 1,2-dipalmitoyl-3-acyl-*sn*-glycerols (Kodali et al., 1984). We found that when the 3-acyl chain was short (acetate or butyrate), the structure was a bilayer like that of crystalline diacylglycerol as described by Pascher & Sundell (1981). When the 3-acyl chain was 6–10 carbons in length, a trilayered structure was formed, but with chains of 12–16 carbons in length the structure was similar to the bilayer structure formed by pure saturated triacylglycerols (Jensen & Mabis, 1966; Larson, 1963). We are now examining molecules that have more biological relevance, that is, molecules with unsaturated fatty acyl chains. In the present study we examined a homologous series of 1,2-dioleoyl-3-acyl-*sn*-glycerols. The 3-position was substituted with a series of even-numbered saturated fatty acids from C_{14} to C_{24}. These acylglycerols resemble some of those found in adipose tissue (Sheppard et al., 1978) and seed oils (Kuksis, 1978). Triglycerides with a long saturated chain (arachidic, behenic, or lignoceric acids) at the glycerol *sn*-3 position represent about 12 mol % of the total triglyceride in peanut oils (Myher et al., 1977; Manganaro et al., 1981). The biological significance of these types of triglycerides is demonstrated by the observations that the atherogenicity of peanut oil fed to rabbits (Manganaro et al., 1981; Kritchevsky et al., 1973) or vervet monkeys (Kritchevsky et al., 1982) was alleviated if the peanut oil triglyceride fatty acids were randomized by interesterification. The 1,2-dioleoyl-3-acyl-*sn*-glycerols (C_{14}–C_{24}) are currently being used to define the

† This work was supported by NIH Grants HL26335 and HL07291.

‡ D.A. is an Established Investigator of the American Heart Association.

0006-2960/85/0424-3757$01.50/0

effects of triglyceride structure on intestinal fat absorption, chylomicron metabolism, and the development of arteriosclerosis (T. G. Redgrave and D. R. Kodali, unpublished results). In the present paper, systematic thermal and X-ray diffraction studies of these compounds are used to describe their structure and their polymorphic behavior.

Materials and Methods

Fatty acids (99% purity) were purchased from Sigma Chemical Co. (St. Louis, MO). 4-(Dimethylamino)pyridine and *N*,*N*'-dicyclohexylcarbodiimide were obtained from Aldrich Chemical Co. (Milwaukee, WI). Solvents [high-pressure liquid chromatography (HPLC)[1] grade] were obtained from Fisher Scientific Co. (Medford, MA). Silicic acid (100–200 mesh) was obtained from Alltech Associates (Deerfield, IL).

Synthesis. The 3-acyl-*sn*-glycerols were prepared according to the procedure reported earlier (Kodali et al., 1985). One mole of each monoacylglycerol in the series from 3-myristoyl- to 3-lignoceroyl-*sn*-glycerol was esterified with 2 mol of oleic acid in the presence of 4-(dimethylamino)pyridine and *N*,*N*'-dicyclohexylcarbodiimide (Kodali et al., 1984) to give the final compounds 1,2-dioleoyl-3-acyl-*sn*-glycerols. These compounds were purified by column chromatography under pressure (Still et al., 1978) on silica gel by elution with a solvent gradient from hexane to hexane/isopropyl ether, 90/10 (v/v). Optical rotation measurements on the 3-acyl-*sn*-glycerols showed no evidence of acyl migration. The structures and purities of the 3-acyl-*sn*-glycerols and 1,2-dioleoyl-3-acyl-*sn*-glycerols were checked by thin-layer chromatography (TLC), high-pressure liquid chromatography (HPLC), and ^{13}C NMR. No evidence of acyl migration was found.

Thin-layer chromatography (TLC) was done on Silica gel "H" plates (250 μm thick) (Analabs, North Haven, CT). The purity of the monoacylglycerols was checked on 2.5% boric acid impregnated TLC plates with the solvent system chloroform/acetone, 75/25 (v/v). All of the intermediate 3-acyl-*sn*-glycerols showed a single spot on TLC without any 2-acylglycerols. Each of the 1,2-dioleoyl-3-acyl-*sn*-glycerols showed a single spot on TLC with the solvent system hexane/isopropyl ether, 75/25 (v/v).

High-pressure liquid chromatograms were obtained on a Varian 5000 liquid chromatograph (Varian Associates, Palo Alto, CA) using an Altex C18-bonded column (4.6 mm × 25 cm) (Rainin Instrument Co. Inc., Woburn, MA). A gradient elution profile was employed from the initial composition of tetrahydrofuran/water/2-propanol/acetonitrile of 5/3/29/63 (by volume) to a final composition of 5/0/55/40. The solvent flow rate was 1.3 mL/min, and the chart speed was 0.25 cm/min. UV detection was employed at 213 nm.

Separate injections of each 1,2-dioleoyl-3-acyl-*sn*-glycerol showed a single peak. The retention times were 22.1, 24.7, 28.6, 32.5, 36.4, and 40.8 min for the 3-myristoyl-, 3-palmitoyl-, 3-stearoyl-, 3-arachidoyl-, 3-behenoyl-, and 3-lignoceroyl-substituted compounds of 1,2-dioleoyl-3-acyl-*sn*-glycerol, respectively.

The ^{13}C NMR spectra were taken in deuterated chloroform at 30 °C with tetramethylsilane as the internal standard on a Bruker 200-MHz spectrometer. The spectra corresponded to pure triacylglycerols, and no contaminant peaks were seen.

[1] Abbreviations: HPLC, high-pressure liquid chromatography; TLC, thin-layer chromatography; ^{13}C NMR, carbon-13 nuclear magnetic resonance; DSC, differential scanning calorimetry; T_f, the peak temperature of the endotherm corresponding to melting of the highest melting polymorph; T_c, the temperature of onset of the crystallization exotherm; ΔH_f, enthalpy of fusion; ΔH_c, enthalpy of crystallization; ΔS, change in entropy.

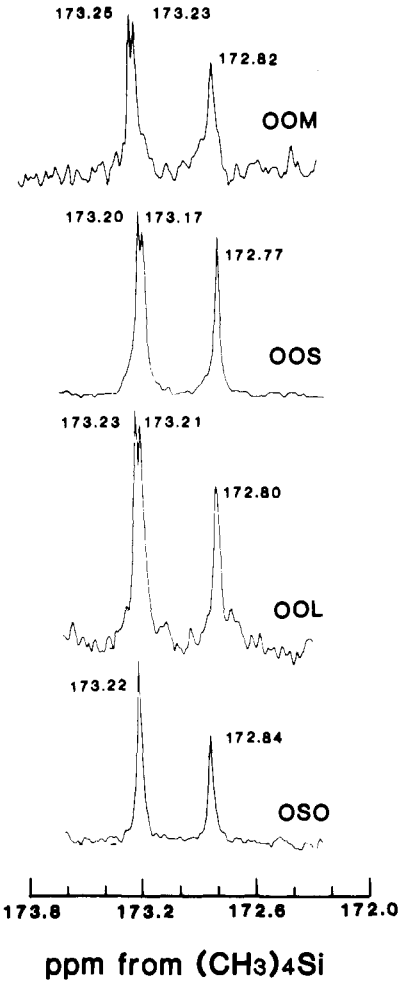

FIGURE 1: ^{13}C NMR tracings of the carbonyl region for the 3-myristoyl (OOM), 3-stearoyl (OOS), and 3-lignoceroyl (OOL) substitutions of 1,2-dioleoyl-3-acyl-*sn*-glycerol. The double peak in the vicinity of 173.2 ppm is due to the two different acyl chains (saturated and unsaturated at the 1- and 3-positions of the glycerol). There is only a single peak at 173.2 ppm when the oleic acid is at both 1- and 3-positions as in 1,3-dioleoyl-2-stearoylglycerol (OSO).

All the final compounds in the 1,2-dioleoyl-3-acyl-*sn*-glycerol series showed three chemical shifts in the carbonyl region (173.1–172.8) (Figure 1). For the acyl carbonyl esterified at the secondary hydroxyl (at carbon 2) of glycerol, a peak at about 172.8 ppm was present. Expansion of the spectral region in the vicinity of 173.2 ppm for all the final compounds revealed two peaks with a chemical shift difference of ~0.02 ppm due to the two different acyl chains (saturated and unsaturated) esterified at the primary hydroxyls of the glycerol (1- and 3-positions). Note that when oleic acid was esterified in both 1- and 3-positions as in 1,3-dioleoyl-2-stearoyl-*sn*-glycerol, only one peak at 173.22 ppm was present.

Differential Scanning Calorimetry (DSC). Differential scanning calorimetry was carried out on a Perkin-Elmer DSC-2 (Norwalk, CT). Approximately 2 mg of each compound, weighed to the nearest 0.01 mg, was sealed in a stainless steel pan. An empty pan was used as a reference sample. Heating and cooling rates were 5 °C/min unless otherwise specified.

Each sample was exposed to three thermal protocols:

(1) The sample was melted to an isotropic liquid, cooled at 10 °C/min to 50 °C below the melting temperature of the highest melting polymorph (the endotherm peak temperature, T_f), and immediately heated to obtain the initial heating curve. The cooling curve and the temperature at which crystallization

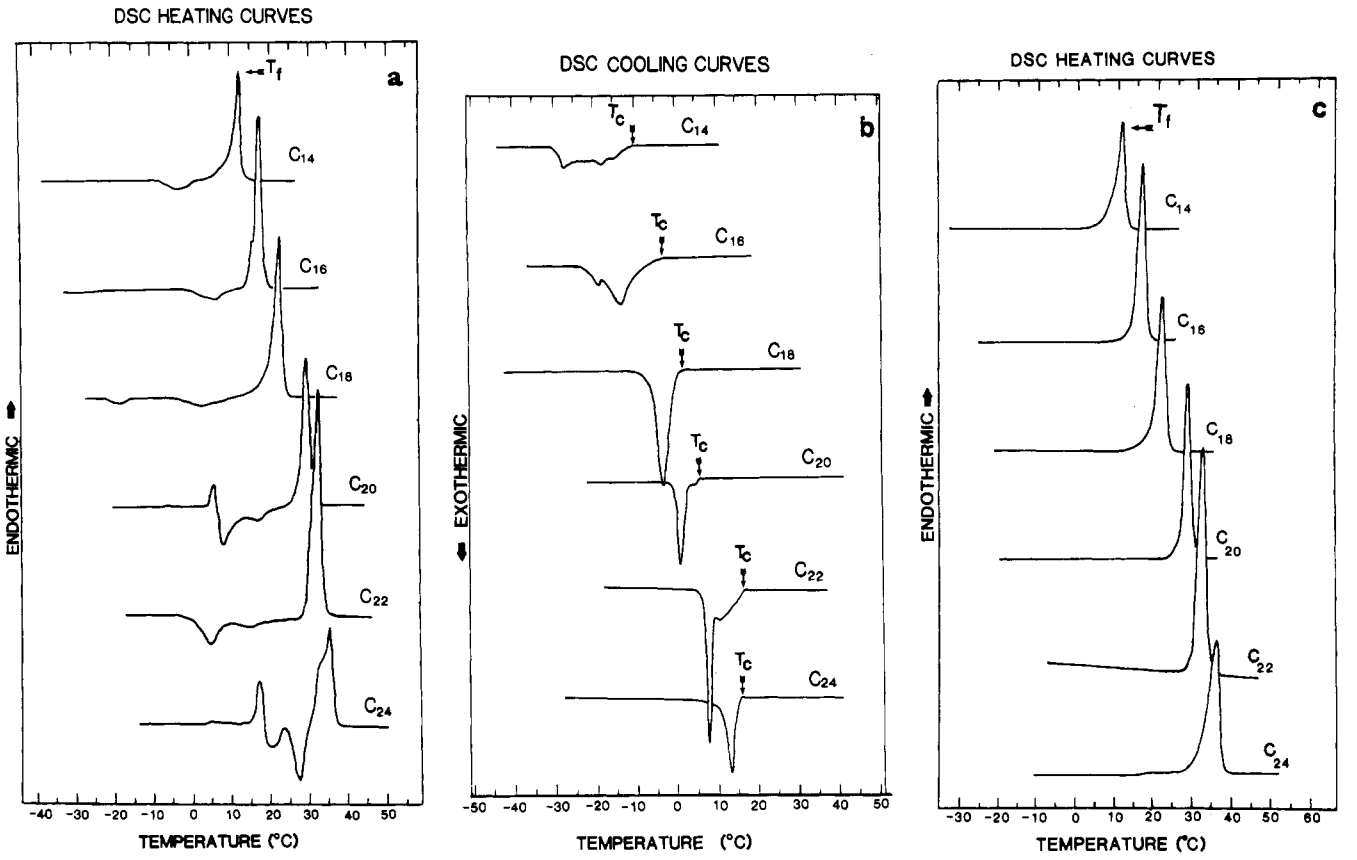

FIGURE 2: (a) DSC heating curves (5 °C/min) taken immediately after heating at 5 °C/min to 15 °C above the melting temperature of the highest melting polymorph, T_f, and cooling at 10 °C/min to 50 °C below T_f (protocol 1). The C_{14} compound exhibits a small exotherm at −2.5 °C and a large endotherm with T_f at 12.0 °C. The C_{16} compound exhibits a small exotherm at 5 °C and a shoulder in the large melting endotherm with T_f at 18.5 °C. The C_{18} compound exhibits two small exotherms at −18 and 2.5 °C and a large endotherm with T_f at 23.2 °C. The C_{20} compound exhibits an endotherm at 5.5 °C followed by two small exotherms and a large endotherm with T_f at 29.8 °C. The C_{22} compound exhibits two exotherms and a large endotherm with T_f at 33.0 °C. The C_{24} compound shows a very small endotherm at 5 °C, an endotherm at 17 °C, and two exotherms at 20 and 27 °C. There is a shoulder in the large melting endotherm with T_f at 36 °C. (b) Cooling curves for the 1,2-dioleoyl-3-acyl-*sn*-glycerols (5 °C/min). The C_{18} and C_{24} compounds recrystallize with single peaks. The other compounds exhibit a double or more complex peak. Recrystallization temperatures (T_c) recorded are those at the onset of recrystallization. (c) DSC heating curves (5 °C/min) after heating the solid to 5 °C below T_f, cooling to 50 °C below T_c, and reheating. All compounds show a single endotherm with a peak temperature identical with the corresponding T_f in Figure 3a.

commenced, T_c, were then obtained.

(2) To attempt to obtain exclusively the highest melting polymorph, the sample was crystallized and then heated to within 5 °C of T_f to melt the low melting polymorphs. To promote growth of the highest melting form, the sample was then cooled to 50 °C below T_f. When the sample was reheated, a single high-melting endotherm was obtained.

(3) To attempt to obtain an α phase (hexagonal chain packing), the sample was cooled to 10–15 °C below T_c and immediately heated. If the crystallization enthalpy was markedly less than the melting enthalpy of the highest melting polymorph, and if upon immediate reheating a single low-temperature endotherm with enthalpy equal to the crystallization enthalpy resulted, we assumed an α phase had crystallized and melted.

The areas under the endotherms and exotherms were measured by planimetry to calculate the enthalpies of fusion (ΔH_f) and enthalpies of crystallization (ΔH_c) by comparing with a known standard enthalpy (indium). The changes in entropy (ΔS) at the melting transition midpoint (T_f) for each compound were calculated by using Gibbs' equation $\Delta S = \Delta H/T_f$.

X-ray Diffraction. X-ray powder diffraction patterns of each sample were recorded by using nickel-filtered Cu Kα radiation from an Elliot GX-6 (Elliot Automation, Borehamwood, U.K.) rotating anode generator equipped with cameras employing Franks double mirror optics (Franks, 1958) and toroidal mirror optics. In special cases a Luzatti-Baro camera with a Tennelec PSD 1100 position-sensitive detector (Tennelec, TN) was also used. The melted compounds were packed into 1-mm diameter Lindeman capillaries (Charles Supper, Natick, MA), sealed, and examined in variable temperature sample holders.

Three protocols, mimicking the DSC protocols, were followed for each sample:

(1) The sample was melted and rapidly cooled to 5 °C, and X-ray diffraction patterns were recorded at 5 °C by using the camera with Franks optics. Exposure time ranged from 24 to 36 h.

(2) The sample was melted, cooled until crystallization was observed, heated, and held within 5 °C of T_f for 5 min. The sample was cooled to 5 °C, and X-ray diffractions were recorded by using the camera with Franks optics. Exposure time ranged from 24 to 36 h.

(3) To attempt to observe the diffraction pattern of an α phase, the melted sample was quenched in acetone–dry ice, and the wide-angle X-ray diffraction pattern was immediately recorded for 30 min at −10 °C by using toroidal mirror optics.

RESULTS

DSC. Figure 2a shows the DSC heating curves for each compound obtained according to DSC protocol 1. For a given

Table I: T, ΔH, and ΔS Values Derived from Figure 2b,c

3-substituent	T_f (°C)[a]	ΔH_f (kcal/mol)[b]	ΔS [cal/(mol K)][c]	T_c (°C)[d]	ΔH_c (kcal/mol)[e]	$T_{f\alpha}$ (°C)[f]	$\Delta H_{f\alpha}$ (kcal/mol)[g]
myristoyl	12.2 ± 0.3[h]	17.9 ± 1.0	62.8 ± 3.6	−10.6 ± 0.6	15.7 ± 0.5		
palmitoyl	18.2 ± 0.4	20.9 ± 1.2	71.8 ± 4.2	−4.0 ± 1.0	17.3 ± 2.4		
stearoyl	22.9 ± 0.2	22.5 ± 1.0	76.0 ± 3.5	2.7 ± 1.0	20.4 ± 1.2		
arachidoyl	29.2 ± 0.7	26.3 ± 0.8	87.0 ± 2.9	6.4 ± 1.7	10.7 ± 0.4		
behenoyl	33.3 ± 0.9	28.1 ± 0.6	91.7 ± 2.3	18.7 ± 4.0	16.0 ± 1.0		
lignoceroyl	36.1 ± 0.3	26.3 ± 2.3	85.1 ± 7.5	15.2 ± 1.0	12.5 ± 3.7	16.5	11.0

[a] Peak temperature of the endotherm corresponding to melting transition of the highest melting polymorph obtained according to DSC protocol 2. [b] Enthalpy of melting transition of highest melting polymorph. Derived from DSC heating curves obtained according to DSC protocol 2. [c] Entropy change associated with melting transition of highest melting polymorph. Calculated from ΔH_f by using Gibbs' equation $\Delta S = \Delta H_f/T_f$. [d] The temperature at which crystallization commenced. [e] Enthalpy of crystallization derived from cooling obtained according to DSC protocol 1. [f] Peak temperature of the endotherm corresponding to melting of the α phase obtained according to DSC protocol 3. [g] Enthalpy of melting transition of α form obtained according to DSC protocol 3. [h] Error value is equal to 2 standard deviations.

Table II: X-ray Powder Diffraction Long and Short Spacings of 1,2-Dioleoyl-3-acyl-*sn*-glycerols after Rapidly Cooling from Isotropic Liquid to 5 °C (X-ray Protocol 1)

	3-substituent					
	14:0 myristoyl	16:0 palmitoyl	18:0 stearoyl	20:0 arachidoyl	22:0 behenoyl	24:0 lignoceroyl
long spacings (Å)	63.7 (s), 2	64.7 (s), 1	67.3 (s), 1	6.93 (s), 1	71.4 (s), 1	70.1 (s), 1
	42.1 (s), 3					
	31.9 (s), 4	32.8 (s), 2	34.1 (s), 2	34.7 (s), 2	35.7 (s), 2	35.2 (s), 2
	21.0 (w), 6	22.3 (w), 3	22.7 (w), 3	23.1 (w), 3	23.8 (w), 3	
	16.0 (w), 8	16.3 (w)8 4	17.1 (w), 4			
	14.1 (w), 9					
	12.7 (w), 10	13.2 (m), 5	13.6 (m), 5	13.8 (m), 5	14.3 (m), 5	14.6 (m), 5
				11.5 (w), 6	12.0 (w), 6	12.1 (w), 6
			8.5 (w), 8			
			7.7 (w), 9		8.0 (w), 9	
		8.2 (w)	7.5 (w)	7.7 (w)	7.6 (w)	
		7.6 (w)	6.8 (w)	5.8 (w)		
short spacings (Å)	4.18 (s)	4.23 (s)	4.51 (w)	4.45 (w)	4.43 (w)	4.50 (w)
	3.89 (s)	3.89 (s)	4.44 (w)	4.17 (s)	4.15 (s)	4.17 (s)
			4.29 (s)	3.78 (s)	3.84 (s)	3.75 (s)
			4.18 (w)			
			4.10 (w)			
			3.87 (s)			

compound the curve was quite reproducible. Although there are some similarities, each compound was different from the others. The variable and often complex thermal behavior indicated that the compounds exhibit varying and often complex polymorphism. When cooled from the isotropic liquid (Figure 2b), the compounds exhibited undercooling, with the difference beteen T_f and T_c ranging from 17 to 24 °C. The C_{18} and C_{24} compounds crystallized with a single peak. The other compounds exhibited an extra peak or shoulder in the crystallization exotherm.

Figure 2c shows the heating curves obtained according to DSC protocol 2. Upon final heating all the triacylglycerols exhibited a single high-temperature endotherm, indicating this protocol was successful in nucleating and growing the high-melting polymorph.

Table I contains T_f, T_c, ΔH_f, ΔH_c, and ΔS values derived from Figure 2b,c. Melting temperatures of the highest melting polymorph range from 12.0 °C for 1,2-dioleoyl-3-myristoyl-*sn*-glycerol to 36 °C for 1,2-dioleoyl-3-lignoceroyl-*sn*-glycerol.

Parts a and b of Figure 3 show heating and cooling curves for the C_{24} compound obtained according to DSC protocol 3. Cooling produced a crystallization at T_c. Immediate heating showed a single low-melting endotherm at $T_{f\alpha}$. The difference between $T_{f\alpha}$ and T_c is 1 °C (Table I). The peak temperature, $T_{f\alpha}$, and the enthalpy, $\Delta H_{f\alpha}$, of the single low-temperature endotherm are given in Table I. If the compound was cooled again (Figure 3c) and held at 15 °C below T_c for 10 min, the subsequent heating curve (Figure 3d) is quite different. Now it is similar to the heating curve obtained according to DSC protocol 1 (Figure 2a, bottom). A single low-temperature

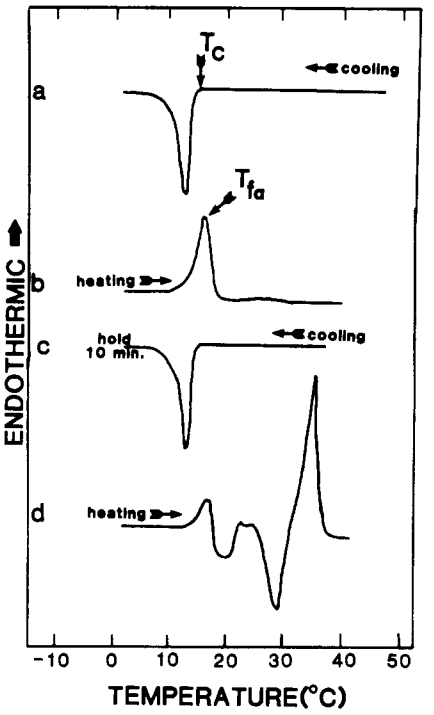

FIGURE 3: Heating and cooling curves (a and b) for 1,2-dioleoyl-3-lignoceroyl-*sn*-glycerol obtained according to DSC protocol 3. If the temperature is held at 15 °C below T_c for 10 min (c), the subsequent heating curve (d) is similar to the heating curve obtained according to DSC protocol 1. A single low-temperature endotherm from compounds other than the C_{24} triacylglycerol could not be obtained by following DSC protocol 3.

Table III: X-ray Powder Diffraction Long and Short Spacings of 1,2-Dioleoyl-3-acyl-*sn*-glycerols after Heating to within 5 °C of the Melting Temperature of the Highest Melting Polymorph (X-ray Protocol 2)

	3-substituent					
	14:0 myristoyl	16:0 palmitoyl	18:0 stearoyl	20:0 arachidoyl	22:0 behenoyl	24:0 lignoceroyl
long spacings (Å)	63.7 (s), 1[a]	65.4 (s), 2	67.3 (s), 1	66.5 (s), 1	71.4 (s), 1	71.3 (s), 1
		43.6 (w), 3				36.8 (w)
	31.9 (s), 2	32.7 (s), 4	34.2 (s), 2	33.2 (s), 2	35.9 (s), 2	35.2 (s), 2
	21.1 (m), 3	21.8 (m), 6	22.7 (w), 3	22.2 (w), 3	24.1 (w), 3	
	15.9 (m), 4	16.4 (m), 8	17.0 (w), 4	16.2 (w), 4		16.4 (w), 4
						14.8 (vw)
	12.7 (m), 5	13.1 (m), 10	13.6 (m), 5	13.4 (m), 5	14.4 (m), 5	14.1 (m), 5
					12.0 (w), 6	11.7 (w), 6
	8.0 (w), 8	8.2 (w), 16	8.5 (w), 8			
	7.7 (vw)	7.7 (w)	7.7 (w)		8.0 (w)	8.2 (w)
		7.6 (w)	7.5 (w)		7.6 (w)	7.8 (w)
	5.8 (w), 11	6.0 (w), 22				
short spacings (Å)	4.50 (w)	4.48 (w)	4.47 (m)	4.51 (m)	4.44 (m)	4.67 (w)
	4.31 (m)	4.41 (w)	4.27 (s)	4.31 (w)	4.23 (s)	4.57 (w)
	4.08 (w)	4.35 (m)	4.17 (w)	4.11 (w)	4.05 (m)	4.51 (s)
	3.90 (s)	4.26 (m)	4.07 (m)	4.05 (w)	3.84 (s)	4.34 (m)
		4.17 (s)	3.87 (s)	3.91 (w)		4.24 (w)
		4.06 (m)			3.85 (w)	4.17 (w)
		3.95 (m)				4.11 (w)
		3.87 (s)				4.07 (w)
						3.92 (w)
						3.86 (m)
						3.78 (w)
						3.67 (w)

[a] Indicates the order of the long spacing.

endotherm from compounds other than the C_{24} triacylglycerol could not be obtained by following DSC protocol 3.

X-ray Diffraction. Diffraction data obtained according to X-ray protocol 1 are given in Table II. The C_{14} compound shows strong diffraction at 1/63.7, 1/42.1, and 1/31.9 Å^{-1}. The strong ca. 1/42 Å^{-1} diffraction is absent in all other compounds. A weak diffraction observed at 1/14.1 Å^{-1} was also not observed in the other compounds. The 1/42 Å^{-1} diffraction together with the weak 1/14.1 Å^{-1} diffraction may be indexed as the $d_{0,0,3}$ and $d_{0,0,9}$ diffractions, respectively from a 126 Å d spacing. The C_{14} compound showed a weak $d_{0,0,1}$ reflection that was partially obscured by the beam stop. The $d_{0,0,6}$, $d_{0,0,8}$, and $d_{0,0,10}$ reflections were also weak, and the $d_{0,0,5}$ and $d_{0,0,7}$ reflections were absent. The C_{16}–C_{24} compounds do not show diffractions ca. 1/42 and ca. 1/14 Å^{-1}. Therefore, the diffractions may be indexed according to a $d_{0,0,1}$ spacing in the range 65–72 Å. The $d_{0,0,1}$ spacings increase from 64.7 Å for the C_{16} compound to 71.4 Å for the C_{22} compound. The $d_{0,0,1}$ spacing is 70.1 Å for the C_{24} compound. The $d_{0,0,2}$ reflections are strong for the C_{16}–C_{24} compounds. The $d_{0,0,3}$ reflections are weak for the C_{16}–C_{24} compounds and is absent for the C_{24} compound. The $d_{0,0,4}$ reflections are weak for the C_{16} and C_{18} compounds and are absent for the C_{20}–C_{24} compounds. The $d_{0,0,5}$ reflections are medium for the C_{16}–C_{24} compounds. The C_{20}–C_{24} compounds have weak $d_{0,0,6}$ reflections that are absent for the C_{16} and C_{18} compounds. A weak $d_{0,0,8}$ reflection was seen for the C_{18} compound, and weak $d_{0,0,9}$ reflections were seen for the C_{18} and C_{22} compounds. The weak diffractions at 1/8.2 and 1/7.6 Å^{-1} for the C_{16} compound, at 1/7.5 and 1/6.8 Å^{-1} for the C_{18} compound, at 1/7.7 and 1/5.8 Å^{-1} for the C_{20} compound, and at 1/7.6 Å^{-1} for the C_{22} compound could not be indexed as a 0,0,l diffraction.

The wide-angle data show strong diffractions at ca. 1/4.2 and 1/3.8 Å^{-1} for all of the compounds. The C_{18}–C_{24} compounds show weak diffractions at ca. 1/4.5 Å^{-1}. The C_{18} compound has additional weak diffractions at 1/4.44, 1/4.18, and 1/4.10 Å^{-1}.

Diffraction data obtained according to X-ray protocol 2 are given in Table III. In this case the C_{16} compound shows a weak diffraction at 1/43.6 Å^{-1} which may be indexed as the $d_{0,0,3}$ diffraction from a 130.8 Å d spacing. The diffraction pattern contained a weak $d_{0,0,1}$ reflection that was partially obscured by the beam stop. The C_{16} compound shows strong $d_{0,0,2}$ and $d_{0,0,4}$ reflections, medium $d_{0,0,6}$, $d_{0,0,8}$, and $d_{0,0,10}$ reflections weak $d_{0,0,16}$ and $d_{0,0,22}$ reflections, and absent reflections from odd 0,0,h planes except the $d_{0,0,3}$ plane.

The C_{14} and C_{18}–C_{24} compounds show no diffraction at ca. 1/42 Å^{-1}, and in all cases the diffraction pattern could be indexed according to a $d_{0,0,1}$ in the range 63–72 Å. The long spacings increase as the 3-acyl chain is lengthened except for the C_{20} and C_{24} compounds. The C_{14} and C_{18}–C_{24} compounds have strong $d_{0,0,1}$ and $d_{0,0,2}$ reflections and medium $d_{0,0,5}$ reflections. The C_{24} compound shows two pairs of closely spaced diffraction lines at ca. 1/36 and 1/14.5 Å^{-1}. The C_{14} compound has a medium $d_{0,0,3}$ reflection while the C_{18}–C_{22} compounds have weak $d_{0,0,3}$ reflections. The $d_{0,0,3}$ reflection is absent for the C_{24} compound. The C_{14} compound has a medium $d_{0,0,4}$ reflection while the C_{18}, C_{20}, and C_{24} compounds have weak $d_{0,0,4}$ reflections. The $d_{0,0,4}$ reflection is absent in the C_{22} compound. All compounds have medium $d_{0,0,5}$ reflections. The C_{22} and C_{24} compounds have weak $d_{0,0,6}$ reflections, and the C_{14} and C_{18} compounds have weak $d_{0,0,8}$ reflections. The C_{14} compound has a weak $d_{0,0,11}$ reflection. The C_{16}–C_{24} compounds each have a pair of diffractions at ca. 1/7 and ca. 1/8 Å^{-1} which could not be indexed as 0,0,l reflections. The C_{14} compound also has one which could not be indexed.

The wide-angle diffraction patterns show that the diffractions at ca. 1/4.5 Å^{-1} are weak for the C_{14} and C_{16} compounds, medium for the C_{18}–C_{22} compounds, and strong for the C_{24} compound. Diffractions at ca. 1/4.2 Å^{-1} are medium for the C_{14} compound, strong for the C_{16}–C_{22} compounds, and weak or absent for the C_{20} and C_{24} compounds. Diffractions at ca. 1/3.8 Å^{-1} are strong for the C_{14}–C_{18} and C_{22} compounds, weak for the C_{20} compound, and medium for the C_{24} compound.

Wide-angle diffraction data obtained according to X-ray protocol 3 showed strong to medium reflections at ca. 1/4.2 and 1/3.8 Å^{-1} for all of the compounds in the series. None

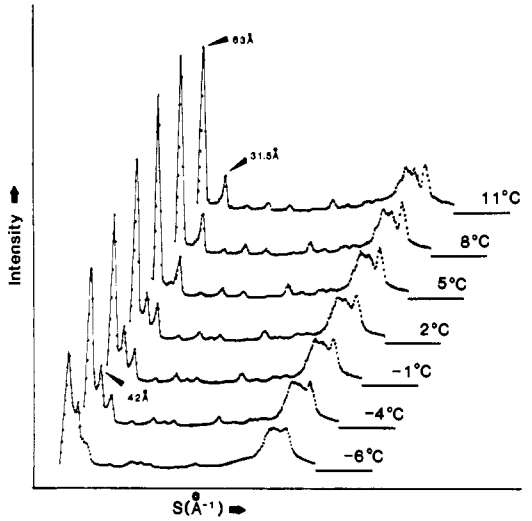

FIGURE 4: Seven 15-min Luzatti-Baro diffraction patterns taken while warming 1,2-dioleoyl-3-myristoyl-*sn*-glycerol from −6 to 11 °C. Note that the 42 Å reflection is gone at 5 °C, indicating a transition from a six-layered to a three-layered structure.

of the compounds showed spacings characteristic of an α phase (single 1/4.1 $Å^{-1}$ diffraction).

To investigate the apparent 126 Å repeat structure observed for the C_{14} compound following rapid cooling (protocol 1), but not observed in protocol 2 used to obtain the stable polymorph, the temperature dependence of the diffraction pattern of the C_{14} compound was further investigated. A Luzatti-Baro camera and position-sensitive detector were used to record the diffraction pattern as a function of temperature. Figure 4 shows seven 15-min exposures taken while warming 1,2-dioleoyl-3-myristoyl-*sn*-glycerol from −6 to 11 °C. Between 2 and 5 °C the $d_{0,0,3}$ at ca. 1/42 $Å^{-1}$ reflection which characterizes the 126 Å repeat structure disappears.

Discussion

The polymorphic form of each compound obtained according to DSC protocol 2 melts with a single high-temperature endotherm with peak temperature T_f. A plot of T_f vs. carbon number (Figure 5a) is approximately linear for the C_{14}–C_{20} triacylglycerols, but T_f values for C_{22} and C_{24} triacylglycerols fall below the line. Plots of ΔH_f and ΔS vs. carbon number (Figure 5b) are also approximately linear throughout the series with slopes of 1.0 kcal/mol per carbon atom and 2.6 cal/(mol K) per carbon atom, respectively. These values indicate that the saturated chains are packed in a well-ordered tightly packed lattice (Small, 1981; Small, 1985b). While it is difficult to prove that the saturated chain subcell is isostructural, the fact that the intensity of the 1/4.5 $Å^{-1}$ diffraction increases with increasing chain length (see Table III) does suggest that these chains have a predominantly β subcell.

DSC protocol 3 demonstrated that the putative α form for the C_{24} compound at 10–15 °C below T_c persisted only for a few minutes (Figure 3a–d). A comparable low-temperature low-enthalpy endotherm could not be demonstrated for the C_{14}–C_{22} triacylglycerols. This putative α form is probably extremely transient in these compounds with shorter saturated chains because crystallization is driven by the oleic chains for which an α form is unfavorable due to the cis double bond kink. Additionally, a single spacing ca. 4.1 Å, characteristic of the α phase, was not seen by X-ray diffraction with X-ray protocol 3, verifying the extremely transient nature of this form.

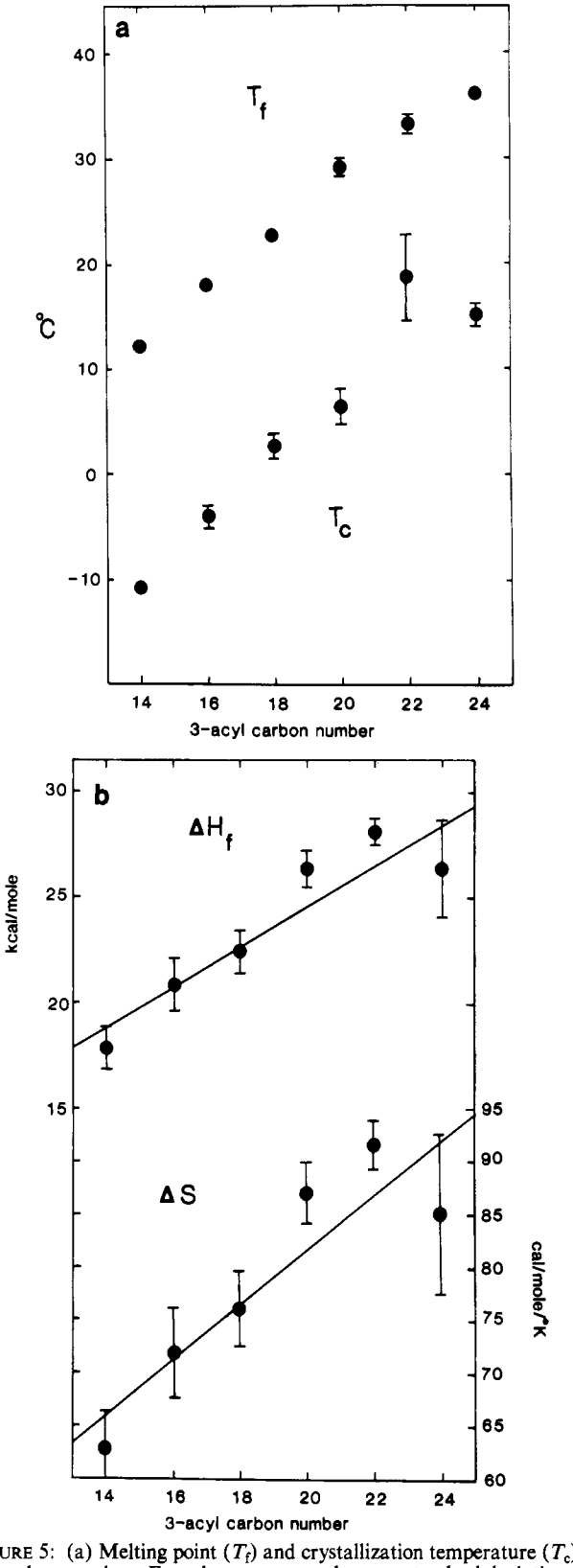

FIGURE 5: (a) Melting point (T_f) and crystallization temperature (T_c) vs. carbon number. Error bars correspond to two standard deviations. (b) Enthalpy (ΔH_f) and entropy (ΔS) of stable high-melting transition vs. carbon number. The slopes are 1.0 kcal/mol per carbon atom and 2.6 cal/(mol K) per carbon atom, respectively.

The DSC heating curves obtained after melting and rapid cooling (DSC protocol 1) (Figure 2a) all have some heat changes similar to the heating curve obtained with the C_{24} compound. The heating curve for the C_{24} compound indicates at least three major polymorphic forms. The small endotherm

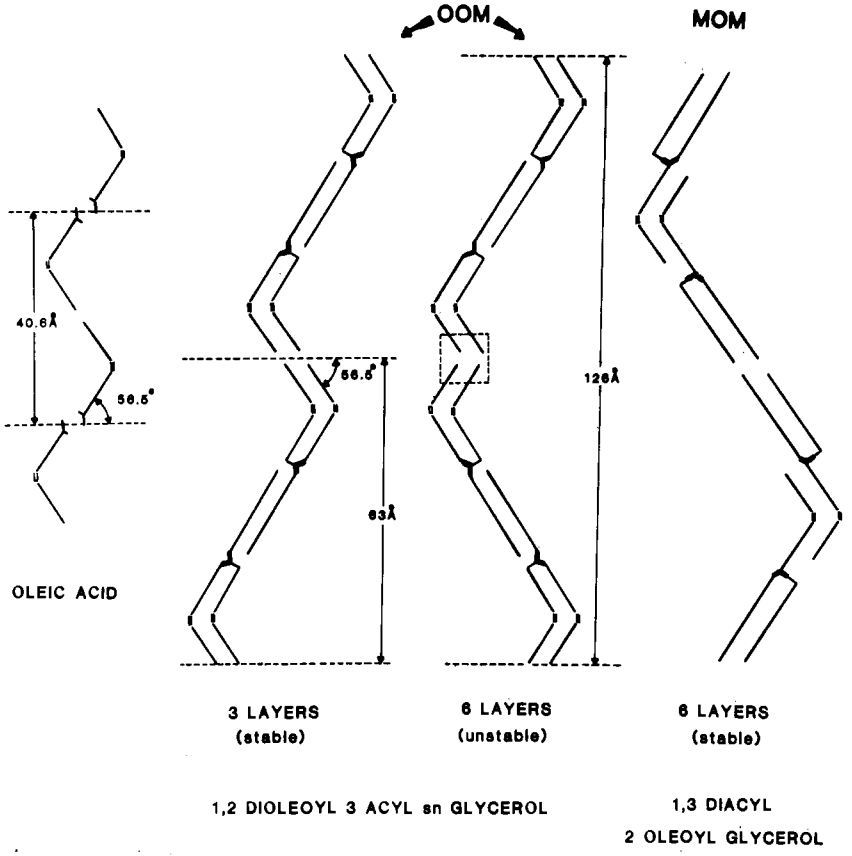

FIGURE 6: Proposed three- and six-layer packing arrangement for the 1,2-dioleoyl-3-acyl-*sn*-glycerols and the 2-oleoyl 1,3-disaturated glycerols. These structures correctly predict that the monosaturated compound (stable form) forms a trilayer whereas the disaturated compound (stable form) forms a six-layered structure. Powder diffraction of 2-oleoyl 1,3-disaturated glycerols was done by Filer et al. (1946). The single crystal structure of oleic acid (left) was determined by Abrahamsson & Ryderstedt-Nahringbauer (1962).

at 4 °C and the shoulder in the 36 °C endotherm indicate two additional polymorphic forms. In general the C_{14}–C_{22} compounds do not show as many polymorphic transitions as the C_{24} compound possibly because the corresponding crystal forms are too unstable or do not nucleate under these conditions. Similar variability in DSC heating curves are seen for saturated mixed chain triglycerides (Kodali et al., 1984). Wide angle X-ray diffraction data suggests predominantly β' subcell packing for all compounds subject to this thermal protocol (X-ray protocol 1) (Table II). However, the weak diffractions at ca. 1/4.5 $Å^{-1}$ suggest a small amount of β packing for the C_{18}–C_{24} compounds.

When heated to within 5 °C of T_f (X-ray protocol 2) (Table III), the C_{20} and C_{24} compounds show β subcell packing (relatively strong 1/4.5 $Å^{-1}$ diffraction). The C_{20} compound shows a corresponding decrease in long spacing. When heated to within 5 °C of T_f, the C_{14}–C_{22} compounds show predominantly β' packing characteristics although the reflections at ca. 1/4.5 $Å^{-1}$ are more intense, suggesting that β packing is becoming significant.

Filer et al. (1946) studied symmetric 2-oleoyl 1,3-disaturated triacylglycerols and found two distinct capillary melting points and two sets of short spacings corresponding to β and β' subcells. In addition, they reported two sets of long spacings for each triacylglycerol corresponding to β and β' phases. In all cases Filer reported long spacings consistent with six-layered packing. For example, the 2-oleoyl-1,3-distearoylglyceride was reported to have a long spacing of 130 Å in the β phase and 140 Å in the β' phase. We did not observe two sets of long spacings for each, 1,2-dioleoyl-3-acyl-*sn*-glycerol, except for the C_{20} triacylglycerol which showed long spacings of 69.3 and 66.6 Å when subject to X-rayl protocols 1 and 2, respectively. The reflection at ca. 35 Å for the C_{24} compound subject to X-ray protocol 2 was clearly a double line, suggesting the coexistence of two phases.

The general features of the packing arrangement of these triacylglycerols can be derived from considerations of their long spacings (Table III) and the known crystal structure of oleic acid. The low-melting form of crystalline oleic acid (Abrahamsson & Ryderstedt-Nahringbauer, 1962) is packed in a bilayer whose c axis is 40.6 Å, with the long axis of the molecule parallel to the c axis. The two parts of the molecule on each side of the double bond have equal angles of tilt with respect to the base plane of 56.5° (Figure 6).

The six-layered long spacings vs. the total number of carbon atoms in four saturated chains included in the six layers of the symmetric 2-oleoyl 1,3-disaturated series plotted from Filer's data produce a best-fit line with a slope of 1.00 Å per carbon and a y intercept of 58.0 Å. For the members of the 1,2-dioleoyl-3-acyl-*sn*-glycerol series exhibiting a common β' subcell (C_{14}–C_{18} and C_{22}), the three-layered long spacings (001) plotted vs. the number of carbon atoms in one saturated chain produce a best-fit line with a slope of 1.05 Å per carbon and a y intercept of 48.8 Å. The slope of the best-fit line is taken as an estimate of the increment in long spacing per added CH_2 group from which the angle of tilt of the saturated chain can be calculated. Our data produces a slope of 1.05 Å per CH_2 corresponding to a tilt of 55.8° with respect to the base plane. Filer's β-phase data produces a slope of 1.00 corresponding to a tilt of 51.9° with respect to the base plane. These tilts are close to the value of 56.5° obtained from the single crystal study of oleic acid, suggesting that the saturated chains have nearly the same tilt as the oleoyl chains. The intercept at zero carbon atoms represents the thickness of the oleoyl–

glycerol region from which the thickness of the glycerol alone is obtained by subtracting the 20.3 Å per oleoyl chain determined by Abrahamsson & Ryderstedt-Nahringbauer (1962). Our data give the thickness of the oleoyl–glycerol region in the trilayer as 48.8 Å. Assuming that there are two oleoyl chain lengths (40.6 Å) and two glycerols within the trilayer, a thickness of 4.1 Å per glycerol is derived. The thickness of the oleoyl–glycerol region derived from Filer's data is 58.0 Å. Assuming there are two oleoyl chain lengths and four glycerols within the six-layered structure, a thickness of about 4.3 Å per glycerol is derived.

Figure 6 illustrates the structures derived from the above analysis for the 1,2-dioleoyl-3-acyl-*sn*-glycerols and the 2-oleoyl 1,3-disaturated glycerols of Filer et al. The orientation of the glycerol depends upon whether the chains at the 1- and 2-positions or the chains at the 1- and 3-positions pack together (Kodali et al., 1984). These proposed structures indicate that the monosaturated compound repeats every three layers whereas the disaturated compound repeats every six layers, consistent with the X-ray data obtained in this study and in that of Filer et al. (1946).

The 126 Å long spacing for the C_{14} compound when melted and rapidly cooled (X-ray protocol 1) is indicative of a six-layer repeat structure. However, the C_{14} compound transforms from a six-layered to a three-layered structure (63 Å) when warmed above 5 °C (Figure 6). It is reasonable to propose that the six-layered structure is a metastable state resulting from rapid cooling and that transformation to a more stable three-layered structure requires sufficient thermal motion. However, extremely weak ca. 1/130 and ca. 1/43 $Å^{-1}$ reflections were observed for the C_{16} compound when heated to 5 °C below T_f, which suggests that a stable six-layered structure may be possible, at least for this compound. No indication of a six-layered structure was seen for the C_{18}–C_{24} compounds in this series.

The proposed difference between the six-layered and three-layered arrangements is a 180° rotation at the interlayer apposition of the oleoyl chains (boxed location, Figure 6). The three-layered structure is more stable than the six-layered structure because of greater van der Waals interaction between the terminal carbon atoms at this boxed location. Since the six-layered and the three-layered structures cannot pack together laterally, the rapidly cooled compound may consist of both six-layered domains and three-layered domains. Heating to just under T_f provides the energy for the six-layered domains to make the transition to the more stable three-layered structure. This transition would require a coordinated 180° rotation at the boxed location (Figure 6) throughout each six-layered domain, producing a measurable exotherm. The transition from the six-layered to three-layered structure in the C_{14} compound (Figure 4) may correspond to the exotherm seen in the DSC heating curve at ca. −2 °C (Figure 2a).

In addition to the α-, β'-, and β-phase transitions, the interlayer reorientations described above may also contribute to the complicated polymorphism of these triglycerides.

ACKNOWLEDGMENTS

We thank Dr. James A. Hamilton for his NMR expertise, David Jackson, Ronald P. Corey, and Howard S. Lilly for their technical assistance, and Anne M. Gibbons and Irene Miller for preparation of the manuscript.

Registry No. 1,2-Dioleoyl-3-myristoyl-*sn*-glycerol, 96479-52-6; 1,2-dioleoyl-3-palmitoyl-*sn*-glycerol, 14863-26-4; 1,2-dioleoyl-3-stearoyl-*sn*-glycerol, 79517-06-9; 1,2-dioleoyl-3-arachidoyl-*sn*-glycerol, 79547-80-1; 1,2-dioleoyl-3-behenoyl-*sn*-glycerol, 79547-81-2; 1,2-dioleoyl-3-lignoceroyl-*sn*-glycerol, 79476-79-2.

REFERENCES

Abrahamsson, S., & Ryderstedt-Nahringbauer, I. (1962) *Acta Crystallogr. 15*, 1261.

Bailey, A. E. (1950) *Melting and Solidification of Fats*, pp 117–180, Interscience, New York.

Chapman, D. (1962) *Chem. Rev. 62*, 433.

Filer, L. J., Sidhu, S. S., Daubert, B. F., & Longenecker, H. E. (1946) *J. Am. Oil Chem. Soc. 68*, 167.

Franks, A. (1958) *Br. J. Appl. Phys. 9*, 349.

Jensen, L. H., & Mabis, A. J. (1966) *Acta Crystallogr. 27*, 977.

Kodali, D. R., Atkinson, D., Redgrave, T. G., & Small, D. M. (1984) *J. Am. Oil Chem. Soc. 61*, 1078.

Kodali, D. R., Redgrave, T. G., Small, D. M. & Atkinson, D. (1985) *Biochemistry 24*, 519–525.

Kritchevsky, D., Tepper, S. A., Vesselinovitch, D., & Wissler, R. W. (1973) *Atherosclerosis (Shannon, Irel.) 17*, 225–243.

Kritchevsky, D., Davidson, L. M., Wright, M., Kriek, N. P. J., & duPlessis, J. P. (1982) *Atherosclerosis (Shannon, Irel.) 42*, 53–58.

Kuksis, A. (1978) *Fatty Acids and Glycerides* (Kuksis, A., Ed.) pp 381–442, Plenum Press, New York.

Larsson, K. (1963) *Proc. Chem. Soc. 87*, 87.

Larsson, K. (1964) *Arch. Chem. 23*, 35.

Lutton, E. S. (1946) *Oil Soap (Chicago) 23*, 265.

Lutton, E. S. (1950) *J. Am. Oil Chem. Soc. 27*, 274.

Malkin, T. (1954) *Prog. Chem. Fats Other Lipids, 2*, 1.

Manganaro, F., Myher, J. J., Kuksis, A., & Kritchevsky, D. (1981) *Lipids 16*, 508–517.

Morley, N. H., Kuksis, A., & Buchnea, D. (1974) *Lipids 9*, 481.

Myher, J. J., Marai, L., Kuksis, A., & Kritchevsky, D. (1977) *Lipids 12*, 775–785.

Pascher, I., & Sundell, S. (1981) *J. Mol. Biol. 153*, 791.

Sheppard, A. J., Iverson, I. L., & Weihrauch, J. L. (1978) *Fatty Acids and Glycerides* (Kuksis, A., Ed.) pp 341–380, Plenum Press, New York.

Small, D. M. (1981) *Pure Appl. Chem. 53*, 2095.

Small, D. M. (1985a) *The Physical Chemistry of Lipids. From Alkanes to Phospholipids Chapter* 10, Plenum Press, New York (in press).

Small, D. M. (1985b) *The Physical Chemistry of Lipids. From Alkanes to Phospholipids* Chapter 2, Plenum Press, New York (in press).

Still, W. C., Kahn, M., & Mitra, A. (1978) *J. Org. Chem. 43*, 2923.